SHIP-1 Regulates the Differentiation and Function of Tregs via Inhibiting mTORC1 Activity

Zuochen Du
Chongqing Medical University Affiliated Children's Hospital
Jinzhi Wang
Chongqing Medical University Pediatric College: Chongqing Medical University Affiliated Children's Hospital
Di Yang
Chongqing Medical University Pediatric College: Chongqing Medical University Affiliated Children's Hospital
Xiaoyu Sun
Chongqing Medical University Pediatric College: Chongqing Medical University Affiliated Children's Hospital
Lu Huang
Chongqing Medical University Affiliated Children's Hospital
xinye Tang
Chongqing Medical University Affiliated Children's Hospital
Xingrong Du
St Jude Children's Research Hospital
Hao Shi
St Jude Children's Research Hospital
Heather Miller
National Institutes of Health
Lisa Westerberg
Karolinska Institutet
Yoshimura Akihiko
Keio University School of Medicine Graduate School of Medicine: Keio Gijuku Daigaku Igakubu Daigakuin Igaku Kenkyuka
Chaohong Liu (✉ chaohongliu80@126.com)
Huazhong University of Science and Technology https://orcid.org/0000-0001-7028-4625

Research Article

Keywords: Cell metabolism, Treg cells, SHIP-1, mTOR

Posted Date: January 7th, 2022

DOI: https://doi.org/10.21203/rs.3.rs-1208354/v1

Abstract

Cell metabolism is crucial for orchestrating the differentiation and function of regulatory T cells (Tregs). However, the underlying signaling mechanism that coordinates cell metabolism to regulate Treg activity is not completely understood. As a pivotal molecule in lipid metabolism, the role of SHIP-1 has been studied extensively in B cells and CD4 T cells, yet its regulatory role in Tregs remains unknown. In this study, we generated “SHIP-1 KO mice” that have SHIP-1 specifically deleted in regulatory T cells by crossing $Foxp3^{YFP\text{-}cre}$ mice with $SHIP\text{-}1^{fl/fl}$ mice. Surprisingly, SHIP-1 KO mice had severe autoimmunity with increased Tregs in the thymus and disrupted peripheral T cell homeostasis. Mechanistically, $CD4^{Cre}$ $SHIP\text{-}1^{flox/flox}$ mice were found to have increased Treg precursors and SHIP-1 KO Tregs had reduced migration and stability, which caused decreased Tregs in the spleen. Additionally, the suppressive function of Tregs from SHIP-1 KO mice was diminished, along with their promotion of anti-tumor immunity. Interestingly, the PI3K-mTORC1, but not mTORC2, signaling axis was enhanced in SHIP-1 KO Tregs. *In vivo* treatment of SHIP-1 KO mice with rapamycin rescued the abnormal Treg percentages and peripheral T cell homeostasis, as well as Treg suppressive function. Furthermore, the treatment of wild-type mice with SHIP-1 inhibitor enhanced anti-tumor activity. Our study has revealed a previously unrecognized underlying function of SHIP-1 in Tregs, which highlights the SHIP-1-PI3K-mTORC1 axis that regulates Treg differentiation and function.

Background

Src homology 2 (SH2) domain containing inositol polyphosphate 5-phosphatase 1 (SHIP-1) is a phosphatase that is encoded by the INPP5D gene in humans(1, 2), which is a member of the inositol polyphosphate-5-phosphatase (INPP5) family of proteins. SHIP-1 has an N-terminal SH2 domain, an inositol phosphatase domain, and two C-terminal protein interaction domains. SHIP-1 is expressed exclusively in cells of hematopoietic lineage. Tyrosine phosphorylation recruits SHIP-1 to the plasma membrane, where it hydrolyzes the 5' phosphate from phosphatidylinositol (3, 4, 5)-trisphosphate and inositol-1,3,4,5-tetrakisphosphate, which affects downstream signaling cascades, such as inhibition of Btk and Akt activation(3–6).

The role of SHIP-1 has been studied extensively in lymphocytes, including B and $CD4^+$ T cells. SHIP-1 is a negative regulator of BCR signaling in B cells(7–9). SHIP-1 deficiency in activation-induced cytidine deaminase (AID^+) B cells reduces the IL-10 production of B10 cells, which induces the autoimmune phenotype in $Innp5d^{fl/fl}Aicda^{Cre/+}$ mice(10). SHIP-1 performs inhibitory functions when recruited to the ITIM of FcγRIIB in B cells(11). However, SHIP-1 is indistinguishably recruited to the plasma membrane in the presence or absence of FcγRII colligation after BCR activation, which relies on the intact domain of the C-terminal region of SHIP-1(12, 13).SHIP-1 and SHP-1 function in parallel pathways, the continuous inhibitory signaling pathways from both are essential for maintenance of B cell anergy(14, 15).Chronic BCR occupancy induces biased monophosphorylation of the BCR CD79 ITAM motifs, leading to the phosphorylation of SHIP-1 and downstream Dok-1 that is critical for maintaining B cell anergy(16).

Although SHIP-1 deficient B cells have lower thresholds for antigen(Ag-) and interferon (IFN)-induced activation and spontaneously generate isotype-switched antibodies, they respond poorly in immunization and infection models. SHIP-1 deficient B cells form germinal centers (GCs) and undergo mutation, but they are not properly selected for high-affinity antibodies(17). SHIP-1 and 3'-inositol phosphatase, phosphatase and tensin homologue (PTEN) synergistically suppress B cell lymphoma and are tumor suppressors(18).

Currently, the role of SHIP-1 in Treg cells is not clearly understood. Indeed, SHIP-1 deficiency promotes generation of the thymic Treg cell population. Dok1 and SHIP-1 are essential for development of Tregs(19). Additionally, the colligation of CD3 and CD28 activates the SHIP-1-Dok2-Grb2 signaling complex and recruits SHIP-1 from the cytosol to the membrane(20,21). Mice with a germ-line deletion of SHIP-1 have an increased number of regulatory T cells(19). But the number of regulatory T cells in the spleen of *CD4^{cre}SHIP-1$^{fl/fl}$* mice are similar to that of wild-type mice(22). *CD4^{cre}SHIP-1$^{fl/fl}$* mice have a reduced humoral immune response, inefficient Th2 skewing and enhanced cytotoxicity(22). *Ex vivo* Tregs from *CD4^{cre}SHIP-1$^{fl/fl}$* mice retained normal suppressive capacity *in vitro* and in a T cell transfer model of colitis(23). Deletion of SHIP-1 reduces the capacity of naive CD4$^+$ T cells to differentiate into Th17 cells and promotes the development of induced Tregs (iTregs)(23). This may indicate that SHIP-1 does not have an essential role in thymic selection or in T cell development in the periphery. In order to resolve this divergence and clarify the role of SHIP-1 in the development and function of Tregs, we performed studies using mice with SHIP-1 knockout only in Tregs .

In this study, we generated SHIP-1 deletion specifically in Tregs by crossing *Foxp3$^{YFP-cre}$* mice with *SHIP-1$^{fl/fl}$* mice. Surprisingly, we found that *Foxp3$^{YFP-cre}$ Ship-1$^{fl/fl}$*mice (referred to as SHIP-1 KO mice for simplicity) had splenomegaly and an autoimmune phenotype characterized by IgG complex deposition in the kidney and increased dsDNA antibodies. The thymic Tregs were significantly increased due to the increase of CD4$^+$ T cells and Treg precursors in the thymus. The loss of SHIP-1 function resulted in increased thymic differentiation but reduced suppressive activity of Treg cells, which led to an enhanced anti-tumor response and altered peripheral homeostasis. We further demonstrated that the function of SHIP-1 in Treg cells is mediated by the downstream PI3K-mTORC1 pathway. Finally, SHIP-1 expression was differentially regulated in Treg cells as compared with conventional T cells (Tconv), indicating that SHIP-1 coordinates the responses of Treg and Tconv cells to promote a productive and self-controlled immune response.

Methods

Mice

Ship-1 conditional knockout mice on a C57/BL6 background were obtained by crossing Foxp3$^{YFP-cre}$ or CD4^{Cre} mice with *SHIP-1*$^{fl/fl}$ mice from Jackson laboratory. All mice were housed in individual ventilated cages within the animal center of the Children's Hospital of Chongqing Medical University. Mice at 8-10 weeks old were used unless otherwise noted. For treatment with rapamycin in vivo, mice were

consecutively injected with rapamycin (4 mg per kg body weight) by IP for 14 days. All animal experiments were performed according to protocols approved by the Institutional Animal Care and Usage Committee of Children's Hospital of Chongqing Medical University.

BM Chimera Mice

For generation of bone marrow chimera mice, CD45.1 mice were irradiated with sublethal radiation (6Gy) and then intravenously injected with 1×10^7 total BM cells containing SHIP-1 KO BM (expressing CD45.2) and WT BM (expressing CD45.1) at a ratio of 1:1. The recipient mice were analyzed after 8 weeks, as described previously(24).

Cell purification and flow cytometry

Lymphocytes from gender-matched *Foxp3*$^{YFP\text{-}cre}$ *Ship-1*$^{fl/fl}$ mice and *Foxp3*$^{YFP\text{-}cre}$ *Ship-1*$^{+/+}$ mice were isolated from the thymus, spleen and lymph nodes according to published protocols(25). For analysis of lymphocyte surface markers, the following antibodies were used: PE anti-ICOS (clone: 7E.17G9, eBioscience), PerCP-anti-7AAD (BBI Life Sciences), PerCP/Cy5.5 anti-CD44 (clone: IM7), APC anti-CD25 (clone: PC61), APC-CY7 anti-TCR-β (clone: H57-597), PE-CY7 anti-CD62L (clone: MEL-14), APC anti-CD304 (Neuropilin-1) (clone: 3E12), Pacific Blue anti-CD4 (clone: RM4-5), Brilliant Violet 510 anti-CD8a (clone: 53-6.7), PE-CY7 anti-PD1 (CD279) (clone: RMP1-30), PE anti-CD4 (clone: GK1.5). All antibodies were from BioLegend unless otherwise stated. For staining cells, antibody incubations were on ice for 30mins in PBS containing 2% FBS. For detection of intracellular proteins, cells were fixed and permeabilized using Foxp3/transcription factor staining buffer set by eBioscience, then stained with the following antibodies: PE anti-CD152 (CTLA - 4) (clone: UC10-4B9), PE anti-Foxp3 (clone: MF-14), APC anti-IL-4 (clone:11B11), PE/Cy7 anti-IFN-γ (clone: XMG1.2), Brilliant Violet 421 anti-IL-17A (clone: TC11-18H10.1). All antibodies were from Biolegend. PE-Cyanine7 Ki-67 monoclonal antibody (SolA15) from eBioscience was used for detecting cell population growth.

Treg cells were sorted using a $CD4^+CD25^+$ regulatory T cell isolation kit (Miltenyi Biotec) and activated in plates coated with anti-CD3 (clone: 145-2C11, Bio X Cell) at 5 mg/ml and anti-CD28 (clone: 37.51, Bio X cell) at 5 mg/ml for 4 hours, then immediately fixed with Phosflow perm buffer (BD Biosciences), permeabilized with Phosflow lyse/fix buffer (BD Biosciences), and stained with: anti-phospho- Akt (pSer 473) (clone: D9E), anti-phospho-S6 (pSer235/236), anti-phospho-PI3 kinase p85 (Tyr458)/p55 (Tyr199), anti-phospho-Foxo1 (Ser256), anti-phospho-mTOR (Ser2448) (clone: D9C2). All antibodies were from Cell Signaling Technology. Flow cytometry data were acquired on a FACS Canto (BD Biosciences) and analyzed using FlowJo software. Cell numbers of various populations were calculated by multiplying the total cell number with the percentages of each individual population from the same mouse, and then averaged.

In vitro Treg suppression assays

For the *in vitro* Treg cell suppression assay, $CD4^+CD25^+$ Treg cells and $CD4^+CD62L^{high}CD44^{low}$ Tnaive cells were sorted by $CD4^+CD25^+$ regulatory T cell and naive $CD4^+$ T cell isolation kits (Miltenyi Biotec), respectively. Tnaive (1×10^5 cells) and Treg cells (at different ratios with Tnaive cells) were cultured in 96-well flat-bottom plates along with anti-CD3 (clone: 145-2C11, Bio X Cell) at 5 mg/ml and anti-CD28 (clone: 37.51, Bio X Cell) at 5 mg/ml for 72 h. T cell proliferation was determined by using the CellTrace violet cell proliferation kit (C34557, Invitrogen). For drug treatment in vitro, Treg cells were preincubated with vehicle or 100 nM rapamycin (AY 2298, MedChemExpress) for 1 h before stimulation.

Colitis model

Colitis model were performed as previously published literature(26).

Tumor model

MC38 colon adenocarcinoma cells were maintained and cultured according to the literature(27), briefly, the MC38 colon adenocarcinoma cells were cultured in DMEM with 10% FBS and 1% penicillin-streptomycin. Gender-matched *Foxp3*$^{YFP-cre}$ *Ship-1*$^{fl/fl}$mice and *Foxp3*$^{YFP-cre}$ *Ship-1*$^{+/+}$ mice were injected subcutaneously with 2 × 105 MC38 colon adenocarcinoma cells in the right flank. Tumors were measured with digital calipers every 3 days, and tumor volumes were calculated by the formula: length × width × (length × width)0.5 × /6. To prepare tumor-infiltrating lymphocytes (TILs), tumors were excised, minced and digested with 0.5 mg/ml collagenase IV (Roche) and 200 U/ml DNase I (Sigma) for 1 h at 37°C. TILs were isolated by density-gradient centrifugation over Percoll (Roche).

In vivo migration ass

$CD4^+$YFP-$Foxp3^+$ Tregs from *Foxp3*$^{YFP-cre}$ *Ship-1*$^{+/+}$ and *Foxp3*$^{YFP-cre}$ *Ship-1*$^{fl/fl}$ mice were respectively transferred into WT $CD45.1^+$ mice, together with B cells from $CD45.2^+$ WT mice for normalization. After 5 hours, the ratio of $CD45.2^+CD4^+$ YFP-$Foxp3^+$ Treg cells vs. $CD45.2^+B220^+$ B cells was analyzed in the spleen, PLN, MLN and blood, and normalized based on the starting ratio 1:2, as previously described(28).

Immunofluorescence analysis

For immunofluorescence staining of mouse kidney sections, the kidneys were embedded in OCT compound and quickly frozen in liquid nitrogen for 1min, then sliced 7 to 10 microns thick. The samples were fixed with cold acetone for 5 min and dried at room temperature. After washing with PBS, the samples were blocked in blocking buffer (5% BSA, 1:100 Fc blocker, in PBS) for 2 hours and stained overnight with AF488 anti-mouse IgG (1:500 in blocking buffer). Images were acquired using confocal microscopy (Nikon A1R).

Serum autoantibody analysis

Autoantibodies to dsDNA were measured with kits from Alpha Diagnostic International.

Quantitative RT-PCR

Splenic $CD4^+$YFP-$Foxp3^+$ Treg cell, CD4SP and CD8SP T cells from WT and $Foxp3^{YFP-cre}$ $Ship\text{-}1^{fl/fl}$, $CD4^{Cre}Ship\text{-}1^{fl/fl}$ mice were sorted on a MoFlow (Beckman-Coulter), then RNA was isolated by RNAPURE kit (RP1202; BioTeke), then the expression of *ship1* were analyzed by using following primers: ship1 F-GCAGCAGATGAAGAACAAG, ship1R- CCAAGTGCCAATGAAGAT.

Statistical analysis.

Statistical significance was assessed by two-tailed unpaired Student's *t*-test with Prism 7 software, ($*p < 0.05$; $**p < 0.01$; $***p < 0.001$). Data are presented as standard error of the mean (SEM).

Results

SHIP-1 reduces the thymic Treg population

In order to study the intrinsic function of SHIP-1 in regulatory T cells, $SHIP\text{-}1^{fl/fl}$ mice were crossed with $Foxp3^{YFP-cre}$ transgenic mice to delete the floxed *SHIP-1* allele specifically in regulatory T cells (SHIP-1 KO mice). The deletion efficiency of $Foxp3^{YFP-cre}$ was examined by RT-PCR and we found that the expression of *ship-1* mRNA was abolished in the regulatory T cells of spleen in SHIP-1 KO mice(Supplementary Figure 1A). The thymuses of SHIP-1 KO mice had increased accumulation of mature single-positive $CD4^+$ (CD4SP) and $CD8^+$ (CD8SP) thymocytes and $CD4^+$YFP-$Foxp3^+$ regulatory T cells compared to $Foxp3^{YFP-Cre}$ $SHIP\text{-}1^{+/+}$ (WT) controls (Figure1A,C,D). To exclude environmental effects, we made WT-WT and WT-SHIP-1 KO bone marrow CD45.1-CD45.2 mixed chimera mice, whereby CD45.1 mice were used as the recipients. After 8 weeks of reconstitution, the mice were euthanized for flow cytometry analysis. The increase of CD4SP and CD8SP thymocytes as well as $Foxp3^+CD4^+$ regulatory T cells in the thymus was also observed in $CD45.2^+$ cells of WT-SHIP-1 KO chimera mice, indicating these results are cell intrinsic (Figure1B). To exclude the deletion leakage of $Foxp3^{YFP-cre}$ in $CD4^+$ and $CD8^+$ T cells, we also examined the mRNA levels of *ship-1* in $CD4^+$ and $CD8^+$ T cells of SHIP-1 KO mice and did not observe difference compare to WT mice(Supplementary Figure 1A). Then we examined the CD45.1 spike cells in WT-SHIP-1 KO chimera mice and found that the percentage of CD45.1 $CD4^+$ and $CD8^+$ T was also increased in thymus compared to that of WT-WT chimera mice(Supplementary Figure 1B). These results suggested that SHIP-1 deletion in Tregs have a dominant effect on the increased accumulation of $CD4^+$ and $CD8^+$ T cells in the thymus. Surprisingly, SHIP-1 KO mice developed profound inflammatory diseases, indicated by reduced body size, hunched posture, and crusting of ears, eyelids and tail (Figure1E). Before dying early in life, SHIP-1 KO mice showed extensive lymphadenopathy and splenomegaly (Figure1E) and infiltrations of lymphocytes and myeloid cells in colon mucosa, lung, liver sinusoids, kidney, and other organs (Figure1F). We also examined the spontaneous generation of GC and T follicular helper cells (Tfh) by flow cytometry, which contributes to the autoimmune phenotype. We found the percentage of GC cells and Tfh cells were significantly increased in SHIP-1 KO mice (Figure1G). Additionally, glomeruli of the

SHIP-1 KO mice kidney contained prominent IgG deposits as systemic autoimmunity is frequently associated with renal pathology (Figure1H). In accordance with this, the titers of dsDNA antibodies were increased in SHIP-1 KO mice (Figure1I). We also examined the expression of SHIP-1 in naïve T cells (Tnaives) and Tregs and found that the expression of SHIP-1 was higher in Tregs compared to Tnaives, which indicated that SHIP-1 may have different and intrinsic roles in Treg function (Supplementary Figure 1C). Altogether, these results suggest that SHIP-1 deficiency causes the expansion of thymic Tregs as well as autoinflammatory disease.

SHIP-1 blocks the differentiation of $CD4^+CD25^+$ $Foxp3^-$ cells into Tregs

We hypothesize that SHIP-1 inhibits the differentiation of Treg precursors ($CD4^+CD25^+Foxp3^-$) into Tregs. It has been shown that $Foxp3^+$ Treg cells develop from precursors that depend on IL-2 and TGF-ß or IL-15 stimulation to express Foxp3, not TCR engagement(29–32). To confirm this, $CD4^{Cre}$ mice were crossed with SHIP-$1^{flox/flox}$ mice to have SHIP-1 specifically deleted in T cells($CD4^{Cre}$ SHIP-$1^{flox/flox}$ mice).Real-time PCR analysis indicated efficient deletion of the *ship-1* gene in thymocytes(Supplementary Figure 1D). Although the number of Tregs in the spleen of $CD4^{Cre}$ SHIP-$1^{flox/flox}$ mice was the same compared to WT mice(22), the thymic Tregs have not been analyzed in $CD4^{Cre}$ SHIP-$1^{flox/flox}$ mice yet. Notably, the $CD4^+CD25^+Foxp3^-$ population was significantly increased in the thymuses of $CD4^{Cre}$ SHIP-$1^{flox/flox}$ mice (Figure2A,B), suggesting that SHIP-1 may act on these cells to restrain further differentiation into mature Foxp3-expressing Treg cells. To investigate whether the accumulation of thymic Tregs is also due to disrupted migration, we examined the role of SHIP-1 in the migration of Treg cells by co-transferring $CD45.2^+$ WT or SHIP-1 deficient Treg cells from SHIP-1 KO mice, together with $CD45.2^+B220^+$ (for normalization) at a 1:2 ratio into $CD45.1^+$ congenic mice. After 5 hours, we found a significant decrease of SHIP-1 deficient Treg cells in the spleen and peripheral and mesenteric lymph nodes, but an increase in the blood, indicating a migration defect of SHIP-1 deficient Treg cells (Figure2C). To further analyze the stability of Tregs, isolated Tregs were labeled with Cell Trace Violet and cultured with anti-CD3+CD28 and IL-2 for 3 days, then analyzed by flow cytometry. More Tregs isolated from SHIP-1 KO mice lost Foxp3 expression upon division in comparison to control WT littermates (Figure2D,E), indicating SHIP-1 is important for the stability of Tregs. Altogether, SHIP-1 blocks the differentiation of $CD4^+CD25^+Foxp3^-$ cells into mature Treg cells and is essential to maintain the stability of Tregs.

SHIP-1 KO Treg cells have altered homeostasis and function

We have shown SHIP-1 negatively regulates thymic differentiation of Treg cells. Whether SHIP-1 also affects the homeostasis and suppressive function of peripheral Treg cells was investigated next. Due to SHIP-1 deficiency on the egress of thymocytes, the amount of CD4SP and CD8SP were significantly decreased in the spleen and peripheral lymph nodes (pLN) of SHIP-1 KO mice (Figure3A,B,C). Although SHIP-1 deficiency resulted in an increased percentage of $Foxp3^+$ CD4SP cells, the total number of $Foxp3^+$ CD4SP cells was decreased in both spleen and pLN (Figure3C). Furthermore, Foxp3 expression on a per cell basis was comparable between WT and SHIP-1 KO cells (Supplementary Figure 2A). In order to confirm that the effect of SHIP-1 deficiency on the altered homeostasis is cell autonomous, we examined the percentage of CD45.2 CD4SP, CD8SP and Tregs in the spleen and pLN. We found that the percentage

of CD45.2 $CD4^+$ and $CD8^+$ T cells was decreased only in the spleen, but not in pLN, and the ratio of CD45.2 Tregs was increased both in spleen and pLN (Figure3D,E). Interestingly the reduction of $CD4^+$ and $CD8^+$ T cells can be observed in CD45.1 spike T cells of WT-SHIP-1 KO chimera mice(Supplementary Figure 2B), which indicates the effect of SHIP-1 deficiency on the reduction of $CD4^+$ and $CD8^+$ T cells is a dominant effect. Altogether these results indicate that the effect of SHIP-1 deficiency on the altered homeostasis of Tregs is cell intrinsic. In SHIP-1 KO spleen and pLN, there was a selective increase of the Treg population marked by the expression of GITR and PD-1 (Figure3F) but not for other markers such as neuropilin, ICOS, CTLA4 and CD103 (Supplementary Figure 2C). For functional studies, we sorted splenic $Foxp3^+$ CD4SP T cells to perform an *in vitro* suppression assay. Proliferation of the target $Foxp3^-$ Tconv cells from wild-type mice was tested in the presence of WT or SHIP-1 deficient $Foxp3^+$ $CD4^+$ Treg cells. SHIP-1 KO Treg cells showed a reduced ability than WT Treg cells to inhibit Tconv cell proliferation (Figure3G). We examined the proliferation and apoptosis of Treg cells alone, but no significant difference was observed in either WT or SHIP-1 KO $Foxp3^+$ cells (Supplementary Figure 2D,E,F,G), suggesting that the difference is not due to the differential proliferation of Treg cells. We further detected the suppression of Treg cells *in vivo* in colitis model, by transferring T_{conv} and Treg cells into *Rag1*$^{-/-}$ mice, after 10 weeks, recipients of T_{conv} and WT Treg mice did not develop colitis, but recipients of T_{conv} and SHIP-1 KO Treg or T_{conv} alone developed obvious colitis (Supplementary Figure 3A-B), and the IFN-γ produced by $CD45.1^+CD4^+$ T cells were significantly decreased in T_{conv} and WT Treg recipients compared with T_{conv} and SHIP-1 KO Treg or T_{conv} alone recipients (Supplementary Figure 3C-D), these results indicating that the ship-1 is essential for Treg cells suppression function. We also examined the central Tregs (cTreg) and effector Tregs (eTreg) by using CD44 and CD62L staining, and we found that the percentage of cTreg and eTreg was not altered in the spleen of SHIP-1 KO mice (Supplementary Figure 3E). Although the percentage of cTreg had no difference, the percentage of eTreg was decreased in the pLN of SHIP-1 KO mice (Supplementary Figure 3F). To determine whether SHIP-1 is required for Treg cells to inhibit anti-tumor immune responses *in vivo*, we inoculated SHIP-1 KO mice with MC38 colon adenocarcinoma cells. Tumor growth was severely suppressed in SHIP-1 KO mice (Figure3H,I), indicating that SHIP-1 KO Treg cells promotes an anti-tumor immune response. Being in line with this result, SHIP-1 KO mice had a significantly increased percentage of tumor-infiltrating $CD8^+$ T cells, but not $CD4^+$ T cells (Figure3J,L) (Supplementary Figure 4A). Additionally, there was an increase in expression of interferon-γ (IFN-γ), IL-4 and IL-17 in effector $CD4^+$and $CD8^+$ T cells (Figure3K,L) (Supplementary Figure 4B,C). However, SHIP-1 KO mice had a profound loss of Treg cells in the tumor site, which could be due to the migration defect of SHIP-1 KO Tregs (Figure3J,L). To examine if SHIP-1 inhibitor can inhibit the tumor *in vivo*, WT mice were injected with SHIP-1 inhibitor for 14 consecutive days and then inoculated with MC38 colon without ceasing the inhibitor injection. Interestingly, we found that the percentage of splenic Tregs was enhanced but the absolute number of Tregs was decreased in WT mice treated with SHIP-1 inhibitor and tumor size was reduced compared to without treatment, although the percentage of $CD4^+$ and $CD8^+$ T cells was not altered (Supplementary Figure 4D,E,F). These results identify a critical role of SHIP-1 in maintaining the homeostasis of Tregs and endowing Treg cells the ability to inhibit anti-tumor immune responses.

The loss of SHIP-1 in Tregs causes autoimmunity

The reduced suppressive function of Treg cells in SHIP-1 KO mice made us speculate whether homeostasis of the immune system was altered in these mice. SHIP-1 KO mice had reduced percentages and numbers of $CD62L^{high}CD44^{low}$ naïve T cells, but increased activated $CD62L^{low}CD44^{high}$ effector and memory T cells in $CD4^+$ and $CD8^+$ T cells in spleen and pLN (Figure4A,B). We also observed an increase of $CD62L^{low}CD44^{high}$ effector and memory T cells in CD45.2 $CD4^+$ and $CD8^+$ T cells (Figure4C), suggesting the increase of memory T cells in SHIP-1 KO mice was cell intrinsic. Furthermore, Tconv cells from SHIP-1 KO mice were hyper-proliferative to TCR stimulation (Figure4D,E), suggesting a lower threshold for activation. Furthermore, we examined cytokine production associated with autoimmune disease.(33) SHIP-1 KO $CD4^+$ and $CD8^+$ T cells produced more IFN-γ, IL-17, IL-2 and IL-4 (Figure4F,G,H,I). Interestingly, the more production of IFN-γ, IL-17 and IL-4 was also observed in CD45.2 $CD4^+$ and $CD8^+$ T cells (Supplementary Figure 5A), showing the increase of inflammatory cytokine productions in SHIP-1 KO mice was cell autonomous. Interestingly we found the production of IFN-γ, IL-17 and IL-4 was also increased in the CD45.1 spike $CD4^+$ and $CD8^+$ T cells of spleen in WT-SHIP-1 KO chimera mice compared to that of WT-WT chimera mice(Supplementary Figure 5B). This indicated that the deficiency of SHIP-1 in Tregs causing more cytokine productions is a dominant effect. Together, the deficiency of SHIP-1 in Treg cells leads to their spontaneous activation and differentiation and breakdown of immune tolerance.

SHIP-1 signaling inhibits mTORC1 to decrease Treg differentiation and function

To investigate mechanisms mediating SHIP-1 function, we stimulated peripheral Tregs with CD3 and CD28 coated plates and determined the phosphorylation levels of mTORC1 and mTORC2 signaling molecules by flow cytometry. We found that the phosphorylation levels of PI3K, S6 and mTOR were significantly enhanced, but that of Foxo-1 and Akt(Ser 473) were not altered in SHIP-1 KO Tregs either in resting or activation state (Figure5A). These results suggest that SHIP-1 may affect the Tregs differentiation by inhibiting the mTORC1 signaling. To test this hypothesis, SHIP-1 KO mice were injected with rapamycin by IP injection for 12 consecutive days and then euthanized for flow cytometry analysis. Interestingly, the frequency of $CD4^+Foxp3^+$T cells in SHIP-1 KO mice treated with rapamycin was reduced to the degree of WT littermates. Furthermore, the percentages of naïve or effector $CD4^+$ and $CD8^+$ T cells were also rescued. And the cytokine productions including IL-4, IL-17 and IFN-γ in $CD44^+$ T cells of SHIP-1 KO mice treated with rapamycin were rescued to the degree of WT mice (Figure5B). Lastly, the suppressive function of SHIP-1 KO Tregs treated with rapamycin was elevated greatly compared to the vehicle treatment (Figure5C). Altogether these results imply that SHIP-1 regulates Treg development and differentiation via inhibiting the mTORC1 activity.

Discussion

Phosphatase activity is generally thought to negatively regulate TCR signaling in the resting or stimulated state. But the role of phosphatase activity is not completely understood in the function of Tregs. Previous

research has shown the deletion of PTEN specifically in Tregs leads to increased Tfh and GC responses as well as inflammatory disease(34). These abnormalities can be rescued by knock-out of INF-γ. Mechanistically, PTEN is critical to maintain Treg stability and metabolic balance between glycolysis and mitochondrial fitness. Moreover, the loss of PTEN enhances mTORC2-Akt activity, and the deficiency of this activity restores PTEN-deficient Treg function. The activity of PI3K is downregulated by two lipid phosphatases: PTEN and SHIP-1. Both hydrolyze PIP3, generating the lipid products, PI4,5P2 and PI3,4P2, respectively. Plasma membrane recruitment of SHIP-1 expressed hematopoietically requires binding of its SH2 domain to proteins with specific phosphotyrosine motifs(35). PTEN, which is expressed ubiquitously and highly active, regulates basal and induced PIP3 levels via dynamic interactions with the plasma membrane(36). It is unknown whether these two phosphatases regulate the Treg differentiation and function in different ways. *Pten$^{fl/fl}$Foxp3-Cre* mice have increased percentages and numbers of Foxp3^{+}Treg cells in the spleen and lymph nodes, spontaneous Tfh and GC formation. *Pten$^{fl/fl}$Foxp3-Cre* Treg cells showed increased levels of ICOS, PD-1, and GITR, but profoundly decreased expression of CD25. Moreover, *Pten$^{fl/fl}$Foxp3-Cre* mice had elevated levels of IFN-γ, but normal IL-17 and IL-4 production. Thus, T cells from *Pten$^{fl/fl}$Foxp3-Cre* mice were spontaneously prone to differentiate into the TH1 phenotype and have more activation of mTORC2 signaling in Treg cells(34). SHIP-1 KO mice also had increased percentages of Foxp3^{+}Treg cells in the spleen and lymph nodes, but reduced number of Tregs in the peripheral lymph node. SHIP-1 KO mice had reduced CD4^{+} cell percentage, increased memory/effector phenotype (CD44^{high}CD62L^{low}) T cells. Further, T cells from SHIP-1 KO mice showed increased IFN-γ, IL-4,IL2 and IL-17 producing CD4^{+} cells and CD8^{+} cells. These phenotypes are reminiscent of those observed in scurfy mice(37). However, the regulation pathway is different in these two mouse models. In *Pten $^{fl/fl}$Foxp3-Cre* Treg cells, mTORC2 activity was upregulated but mTORC1 activity was upregulated in SHIP-1 KO Treg cells. Therefore, we have established another different regulation pathway by SHIP-1 via mTORC1 compared to that of PTEN through mTORC2. To further confirm that SHIP-1 regulates the Tregs via mTORC1, it is urgent to cross *Foxp3$^{YFP\text{-}cre}$ Ship-1$^{fl/fl}$* mice with *Raptor$^{fl/fl}$* mice for confirmation on a genetic level. Additionally, the production of all the cytokines was elevated in SHIP-1 KO mice unlike the Th1 cytokines in *Pten$^{fl/fl}$Foxp3-Cre* mice.

The role of SHIP-1 in the development and function of Tregs remains controversial. By using the germline deletion mice, SHIP-1$^{-/-}$ mice also have an increase in the proportion, but not the absolute number of thymic Foxp3^{+} Tregs. Moreover, T cell-specific deletion of SHIP-1 with CD4-Cre does not result in an increase in the number of splenic Foxp3^{+} cells(22). In SHIP-1 KO mice, the percentage and number of thymic and splenic Foxp3^{+} Tregs were both increased. Wild-type and SHIP-1$^{-/-}$ Tregs suppress Teff cell proliferation in the same degree *in vitro*(23). These results are in line with previous findings that SHIP-1 deficient Tregs retain their suppressive function intact(19, 38). Furthermore, SHIP-1 deficient Tregs in *CD4^{cre}SHIP-1$^{fl/fl}$* mice suppress the adoptive transfer of colitis(23). These results indicate that the suppressive function of SHIP-1 deficient Tregs in germline deletion mice or *CD4^{cre}SHIP-1$^{fl/fl}$* mice is intact. But in our animal model, the suppressive function of SHIP-1 deficient Tregs has a defect both *in vitro and*

in vivo. Considering the deletion specificity and the impact of the environment, our model has precisely explained the effect of SHIP-1 deficiency on the differentiation and function of Tregs.

The mTORC activity is correlated with the function of Tregs. mTORC1 signaling is essential for Treg cell function in mice and enhanced in Treg cells compared to naive T cells. Treg-specific deletion of the signature component of mTORC1-raptor leads to a significantly reduced suppressive activity *in vivo* and inflammatory disorders(39). Our results have also shown that Tregs with higher mTORC1 activity also leads to the diminished suppressive function of Tregs and inflammatory disease. T cells lacking mTORC differentiate into $Foxp3^{+}$ regulatory cells. However, T cells with mTORC1 deletion do not divert to a regulatory T cell pathway, indicating mTORC2 signaling in preventing the generation of regulatory T cells. Altogether these suggest that mTORC1 and mTORC2 signaling regulate decisions between effector and regulatory T cells(40). Foxp3-Cre Raptor KO mice have abolished mTORC1 activity but enhanced mTORC2 activity. However, SHIP-1 KO mice have increased mTORC1 activity, but normal mTORC2 activity. S1P1 transgenic mice have increased mTORC1 activity that promotes the accumulation of Treg precursors-$CD25^{+}$Foxp3- populations, which is in line with the results of $CD4^{Cre}$SHIP-1 $^{flox/flox}$ mice(26).

Conclusion

Our study has established the intrinsic role of SHIP-1 on the development, differentiation and function in Tregs, which is different from what has been previously reported, especially that SHIP-1 is the pivotal positive determinant of Treg-cell function in mice. Furthermore, we have revealed the underlying regulatory molecular mechanism of the SHIP-1-PI3K-mTORC1 axis, which is essential for the differentiation and function of Tregs. More excitingly, the fact that SHIP-1 inhibition increases anti-tumor activity can facilitate the advancement of cancer therapeutic treatment.

Abbreviations

Tregs: Regulatory T cells.

SHIP-1: Src homology 2 (SH2) domain containing inositol polyphosphate 5-phosphatase1

INPP5: inositol polyphosphate-5-phosphatase

Akt: AKT serine/threonine kinase

APC: Allophycocyanin

BM: Bone marrow

FITC: Fluorescein isothiocyanate

GCs: Germinal centers

PTEN: phosphatase and tensin homologue

PI3K: Phosphatidylinositol-4,5-bisphosphate 3-kinase

Tconv: conventional T cells

Foxp3: forkhead box P3

mTOR: mammaliantargetofrapamycin

Declarations

Ethics approval and consent to participate

All animal experiments were performed according to protocols approved by the Institutional Animal Care and Usage Committee of Children's Hospital of Chongqing Medical University.

Consent for publication

Not applicable.

Availability of data and materials

Because of our internal policy, raw data cannot be shared.

Competing interests

The authors declare no potential conflicts of interest with respect to the research, authorship, and/or publication of this article.

Funding

This study was supported by the National Natural Science Foundation of China (81722002 and 81861138002) and a startup funding from Huazhong University of Science and Technology.

Acknowledgments

Thanks for the critical reading of the manuscript by Dr.Xiaoping Zhong from Duke University. C.L. gives thanks to Hongbo Chi for his inculcated mentoring in his postdoctoral studies.

Author Contributions

Z.D. carried out the initial analyses and drafted the initial manuscript. Z.D.,D.Y.,L.H. performed the flow cytometry assay, J.W. performed the chimera and histopathology analysis, Z.D. performed MC38 tumor model and immunofluorescence, H.S.,X.D., X.Z.,L.W.,Y.A. S.G.Z reviewed and revised the manuscript. C.L.

conceptualized and designed the study, reviewed and revised the manuscript. All authors approved the final manuscript as submitted and agree to be accountable for all aspects of the work.

References

1. Damen JE, Liu L, Rosten P, Humphries RK, Jefferson AB, Majerus PW*, et al.* The 145-kDa protein induced to associate with Shc by multiple cytokines is an inositol tetraphosphate and phosphatidylinositol 3,4,5-triphosphate 5-phosphatase. Proceedings of the National Academy of Sciences of the United States of America **1996**;93(4):1689-93.
2. Ware MD, Rosten P, Damen JE, Liu L, Humphries RK, Krystal G. Cloning and characterization of human SHIP, the 145-kD inositol 5-phosphatase that associates with SHC after cytokine stimulation. Blood **1996**;88(8):2833-40.
3. Carver DJ, Aman MJ, Ravichandran KS. SHIP inhibits Akt activation in B cells through regulation of Akt membrane localization. Blood **2000**;96(4):1449-56.
4. Aman MJ, Lamkin TD, Okada H, Kurosaki T, Ravichandran KS. The inositol phosphatase SHIP inhibits Akt/PKB activation in B cells. The Journal of biological chemistry **1998**;273(51):33922-8.
5. Bolland S, Pearse RN, Kurosaki T, Ravetch JV. SHIP modulates immune receptor responses by regulating membrane association of Btk. Immunity **1998**;8(4):509-16.
6. Chacko GW, Tridandapani S, Damen JE, Liu L, Krystal G, Coggeshall KM. Negative signaling in B lymphocytes induces tyrosine phosphorylation of the 145-kDa inositol polyphosphate 5-phosphatase, SHIP. Journal of immunology **1996**;157(6):2234-8.
7. Liu Q, Oliveira-Dos-Santos AJ, Mariathasan S, Bouchard D, Jones J, Sarao R*, et al.* The inositol polyphosphate 5-phosphatase ship is a crucial negative regulator of B cell antigen receptor signaling. The Journal of experimental medicine **1998**;188(7):1333-42.
8. Cui B, Chen L, Zhang S, Mraz M, Fecteau JF, Yu J*, et al.* MicroRNA-155 influences B-cell receptor signaling and associates with aggressive disease in chronic lymphocytic leukemia. Blood **2014**;124(4):546-54 doi 10.1182/blood-2014-03-559690.
9. Ono M, Bolland S, Tempst P, Ravetch JV. Role of the inositol phosphatase SHIP in negative regulation of the immune system by the receptor Fc(gamma)RIIB. Nature **1996**;383(6597):263-6 doi 10.1038/383263a0.
10. Chen Y, Hu F, Dong X, Zhao M, Wang J, Sun X*, et al.* SHIP-1 Deficiency in AID(+) B Cells Leads to the Impaired Function of B10 Cells with Spontaneous Autoimmunity. Journal of immunology **2017**;199(9):3063-73 doi 10.4049/jimmunol.1700138.
11. Isnardi I, Bruhns P, Bismuth G, Fridman WH, Daeron M. The SH2 domain-containing inositol 5-phosphatase SHIP1 is recruited to the intracytoplasmic domain of human FcgammaRIIB and is mandatory for negative regulation of B cell activation. Immunology letters **2006**;104(1-2):156-65 doi 10.1016/j.imlet.2005.11.027.

12. Pauls SD, Ray A, Hou S, Vaughan AT, Cragg MS, Marshall AJ. FcgammaRIIB-Independent Mechanisms Controlling Membrane Localization of the Inhibitory Phosphatase SHIP in Human B Cells. Journal of immunology **2016**;197(5):1587-96 doi 10.4049/jimmunol.1600105.
13. Aman MJ, Walk SF, March ME, Su HP, Carver DJ, Ravichandran KS. Essential role for the C-terminal noncatalytic region of SHIP in FcgammaRIIB1-mediated inhibitory signaling. Molecular and cellular biology **2000**;20(10):3576-89.
14. Getahun A, Beavers NA, Larson SR, Shlomchik MJ, Cambier JC. Continuous inhibitory signaling by both SHP-1 and SHIP-1 pathways is required to maintain unresponsiveness of anergic B cells. The Journal of experimental medicine **2016**;213(5):751-69 doi 10.1084/jem.20150537.
15. Akerlund J, Getahun A, Cambier JC. B cell expression of the SH2-containing inositol 5-phosphatase (SHIP-1) is required to establish anergy to high affinity, proteinacious autoantigens. Journal of autoimmunity **2015**;62:45-54 doi 10.1016/j.jaut.2015.06.007.
16. O'Neill SK, Getahun A, Gauld SB, Merrell KT, Tamir I, Smith MJ*, et al.* Monophosphorylation of CD79a and CD79b ITAM motifs initiates a SHIP-1 phosphatase-mediated inhibitory signaling cascade required for B cell anergy. Immunity **2011**;35(5):746-56 doi 10.1016/j.immuni.2011.10.011.
17. Leung WH, Tarasenko T, Biesova Z, Kole H, Walsh ER, Bolland S. Aberrant antibody affinity selection in SHIP-deficient B cells. European journal of immunology **2013**;43(2):371-81 doi 10.1002/eji.201242809.
18. Miletic AV, Anzelon-Mills AN, Mills DM, Omori SA, Pedersen IM, Shin DM*, et al.* Coordinate suppression of B cell lymphoma by PTEN and SHIP phosphatases. The Journal of experimental medicine **2010**;207(11):2407-20 doi 10.1084/jem.20091962.
19. Kashiwada M, Cattoretti G, McKeag L, Rouse T, Showalter BM, Al-Alem U*, et al.* Downstream of tyrosine kinases-1 and Src homology 2-containing inositol 5'-phosphatase are required for regulation of CD4+CD25+ T cell development. Journal of immunology **2006**;176(7):3958-65.
20. Edmunds C, Parry RV, Burgess SJ, Reaves B, Ward SG. CD28 stimulates tyrosine phosphorylation, cellular redistribution and catalytic activity of the inositol lipid 5-phosphatase SHIP. European journal of immunology **1999**;29(11):3507-15 doi 10.1002/(SICI)1521-4141(199911)29:11<3507::AID-IMMU3507>3.0.CO;2-9.
21. Dong S, Corre B, Foulon E, Dufour E, Veillette A, Acuto O*, et al.* T cell receptor for antigen induces linker for activation of T cell-dependent activation of a negative signaling complex involving Dok-2, SHIP-1, and Grb-2. The Journal of experimental medicine **2006**;203(11):2509-18 doi 10.1084/jem.20060650.
22. Tarasenko T, Kole HK, Chi AW, Mentink-Kane MM, Wynn TA, Bolland S. T cell-specific deletion of the inositol phosphatase SHIP reveals its role in regulating Th1/Th2 and cytotoxic responses. Proc Natl Acad Sci U S A **2007**;104(27):11382-7 doi 10.1073/pnas.0704853104.
23. Locke NR, Patterson SJ, Hamilton MJ, Sly LM, Krystal G, Levings MK. SHIP regulates the reciprocal development of T regulatory and Th17 cells. Journal of immunology **2009**;183(2):975-83 doi 10.4049/jimmunol.0803749.

24. Niu L, Xuan X, Wang J, Li L, Yang D, Jing Y*, et al.* Akt2 Regulates the Differentiation and Function of NKT17 Cells via FoxO-1-ICOS Axis. Front Immunol **2018**;9:1940 doi 10.3389/fimmu.2018.01940.
25. Sharma S, Orlowski G, Song W. Btk regulates B cell receptor-mediated antigen processing and presentation by controlling actin cytoskeleton dynamics in B cells. Journal of immunology (Baltimore, Md : 1950) **2009**;182(1):329-39 doi 10.4049/jimmunol.182.1.329.
26. Liu G, Burns S, Huang G, Boyd K, Proia RL, Flavell RA*, et al.* The receptor S1P1 overrides regulatory T cell-mediated immune suppression through Akt-mTOR. Nat Immunol **2009**;10(7):769-77 doi 10.1038/ni.1743.
27. Wei J, Long L, Yang K, Guy C, Shrestha S, Chen Z*, et al.* Autophagy enforces functional integrity of regulatory T cells by coupling environmental cues and metabolic homeostasis. Nat Immunol **2016**;17(3):277-85 doi 10.1038/ni.3365.
28. Shi H, Liu C, Tan H, Li Y, Nguyen TM, Dhungana Y*, et al.* Hippo Kinases Mst1 and Mst2 Sense and Amplify IL-2R-STAT5 Signaling in Regulatory T Cells to Establish Stable Regulatory Activity. Immunity **2018**;49(5):899-914 e6 doi 10.1016/j.immuni.2018.10.010.
29. Lio CW, Hsieh CS. A two-step process for thymic regulatory T cell development. Immunity **2008**;28(1):100-11 doi 10.1016/j.immuni.2007.11.021.
30. Burchill MA, Yang J, Vang KB, Moon JJ, Chu HH, Lio CW*, et al.* Linked T cell receptor and cytokine signaling govern the development of the regulatory T cell repertoire. Immunity **2008**;28(1):112-21 doi 10.1016/j.immuni.2007.11.022.
31. Zheng SG, Gray JD, Ohtsuka K, Yamagiwa S, Horwitz DA. Generation ex vivo of TGF-beta-producing regulatory T cells from CD4+CD25- precursors. Journal of immunology (Baltimore, Md : 1950) **2002**;169(8):4183-9 doi 10.4049/jimmunol.169.8.4183.
32. Zheng SG, Wang JH, Gray JD, Soucier H, Horwitz DA. Natural and induced CD4+CD25+ cells educate CD4+CD25- cells to develop suppressive activity: the role of IL-2, TGF-beta, and IL-10. Journal of immunology (Baltimore, Md : 1950) **2004**;172(9):5213-21 doi 10.4049/jimmunol.172.9.5213.
33. Theofilopoulos AN, Koundouris S, Kono DH, Lawson BR. The role of IFN-gamma in systemic lupus erythematosus: a challenge to the Th1/Th2 paradigm in autoimmunity. Arthritis Res **2001**;3(3):136-41 doi 10.1186/ar290.
34. Shrestha S, Yang K, Guy C, Vogel P, Neale G, Chi H. Treg cells require the phosphatase PTEN to restrain TH1 and TFH cell responses. Nat Immunol **2015**;16(2):178-87 doi 10.1038/ni.3076.
35. Sattler M, Verma S, Pride YB, Salgia R, Rohrschneider LR, Griffin JD. SHIP1, an SH2 domain containing polyinositol-5-phosphatase, regulates migration through two critical tyrosine residues and forms a novel signaling complex with DOK1 and CRKL. J Biol Chem **2001**;276(4):2451-8 doi 10.1074/jbc.M006250200.
36. Vazquez F, Devreotes P. Regulation of PTEN function as a PIP3 gatekeeper through membrane interaction. Cell Cycle **2006**;5(14):1523-7 doi 10.4161/cc.5.14.3005.
37. Kanangat S, Blair P, Reddy R, Daheshia M, Godfrey V, Rouse BT*, et al.* Disease in the scurfy (sf) mouse is associated with overexpression of cytokine genes. Eur J Immunol **1996**;26(1):161-5 doi

10.1002/eji.1830260125.

38. Collazo MM, Wood D, Paraiso KH, Lund E, Engelman RW, Le CT*, et al.* SHIP limits immunoregulatory capacity in the T-cell compartment. Blood **2009**;113(13):2934-44 doi 10.1182/blood-2008-09-181164.
39. Zeng H, Yang K, Cloer C, Neale G, Vogel P, Chi H. mTORC1 couples immune signals and metabolic programming to establish T(reg)-cell function. Nature **2013**;499(7459):485-90 doi 10.1038/nature12297.
40. Delgoffe GM, Kole TP, Zheng Y, Zarek PE, Matthews KL, Xiao B*, et al.* The mTOR kinase differentially regulates effector and regulatory T cell lineage commitment. Immunity **2009**;30(6):832-44 doi 10.1016/j.immuni.2009.04.014.

Figures

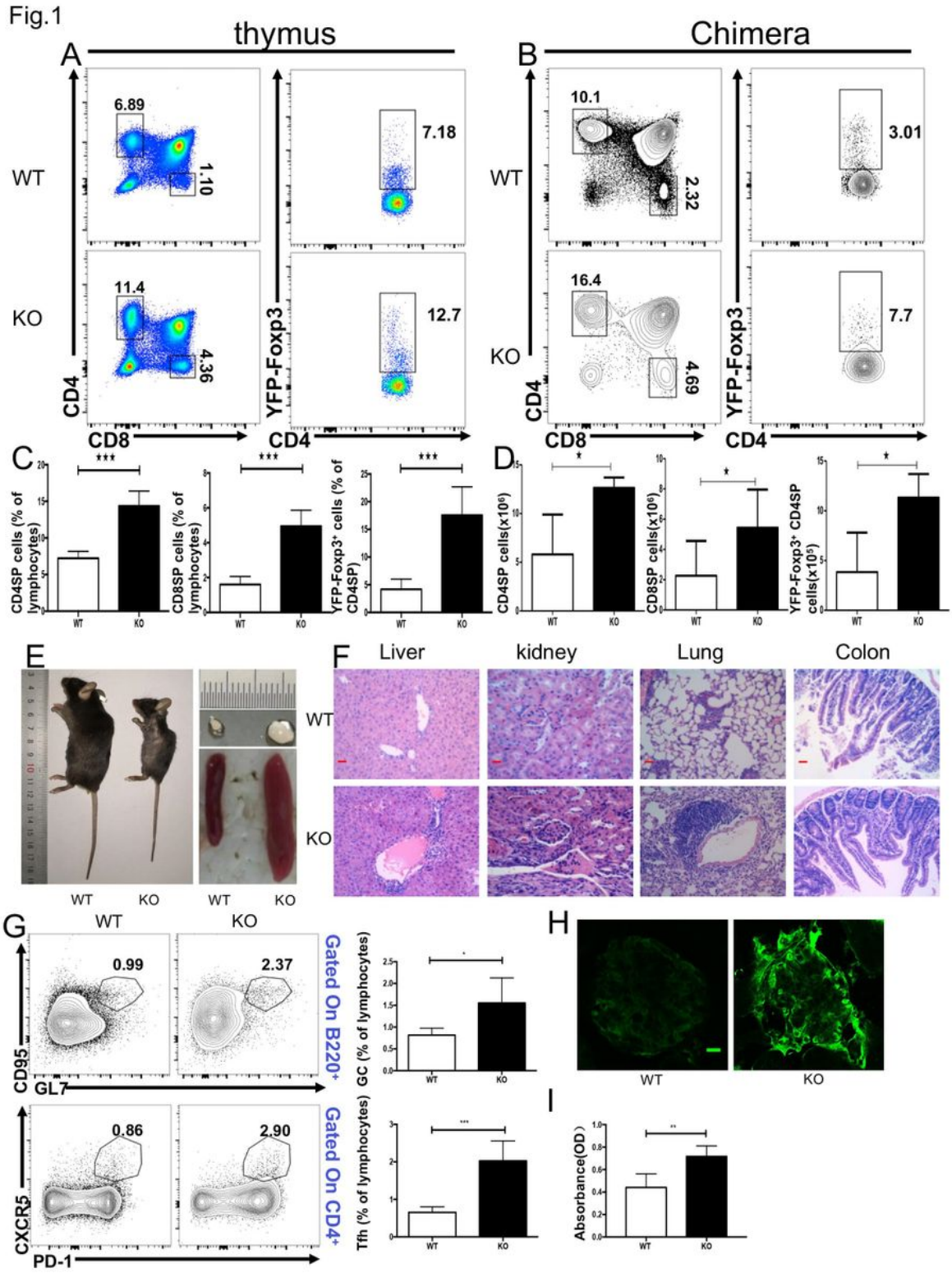

Figure 1

SHIP-1 deficiency increases the thymic Treg population

(A) Flow cytometry data of CD4SP, CD8SP, and CD4^{+}YFP-Foxp3^{+} Treg cells from the thymuses of *Foxp3$^{YFP\text{-}cre}$ Ship-1$^{+/+}$* (WT) and *Foxp3$^{YFP\text{-}cre}$ Ship-1$^{fl/fl}$* (SHIP-1 KO) mice. (B) CD45.1 mice were irradiated with sublethal radiation (6Gy) and then intravenously injected with 1×10^{7} total BM cells containing SHIP-

1 KO BM (expressing CD45.2) and WT BM (expressing CD45.1), at a ratio of 1:1. The CD4SP, CD8SP, and $CD4^+$YFP-$Foxp3^+$Treg cells from the thymuses of recipient mice were analyzed after 8 weeks. (C,D) Percentage and absolute number of selected cell populations from (A) (n=6). (E) Image of 8 weeks-old WT(n=3) and SHIP-1 KO mice as well as spleens and peripheral lymph nodes. (F) Hematoxylin and eosin staining of liver, kidney, lung, and colon from WT and SHIP-1 KO mice. Shown are representative images from 3 mice. Scale bars, 200μm. (G) Flow cytometry data of GC and Tfh cells from spleens of WT (left panel) and SHIP-1 KO (right panel) mice (n=5), and percentages of the selected cell populations. (H) Immunofluorescence showing IgG antibodies deposited in SHIP-1 KO mouse glomeruli. Shown are representative images from 3 mice. Scale bars, 25μm. (I) Titers of anti-nuclear antigen and anti-dsDNA antibodies of WT and SHIP-1 KO mice (n=6).

Figure 2

SHIP-1 blocks differentiation of $CD4^+CD25^+$ Foxp3 cells

(A) Flow cytometry data of $CD4^+CD25^+Foxp3^+$ and $CD4^+CD25^+Foxp3^-$ cells gated from CD4SP thymocytes of WT and $CD4^{Cre}$SHIP-$1^{flox/flox}$ mice. (B) Percentage and absolute number of selected cell populations from (A) (n=6). (C) Sorted $CD4^+$YFP-$Foxp3^+$ Treg cells ($5x10^5$) from WT or SHIP-1 KO mice and B cells ($1x10^6$) from WT mice were adoptively transferred into wild-type congenic $CD45.1^+$ mice (n = 6). After 5 hr, the ratio of $CD45.2^+CD4^+$YFP-$Foxp3^+$ Treg cells vs. $CD45.2^+B220^+$ B cells was analyzed from the spleen, PLN, MLN, and blood, then normalized with the starting ratio before transfer (1:2). (D) Sorted $CD4^+$YFP-$Foxp3^+$Treg cells from spleens of WT(n=3) and SHIP-1 KO mice were labeled with CellTrace Violet, and co-cultured with anti-CD3, anti-CD28, and IL-2 for 5 days. (E) The expression of Foxp3 in $CD4^+$SP from WT (n=3) and SHIP-1 KO mice after co-culture for 5 days with anti-CD3, anti-CD28, and IL-2. Shown were the representative results from three independent experiments.

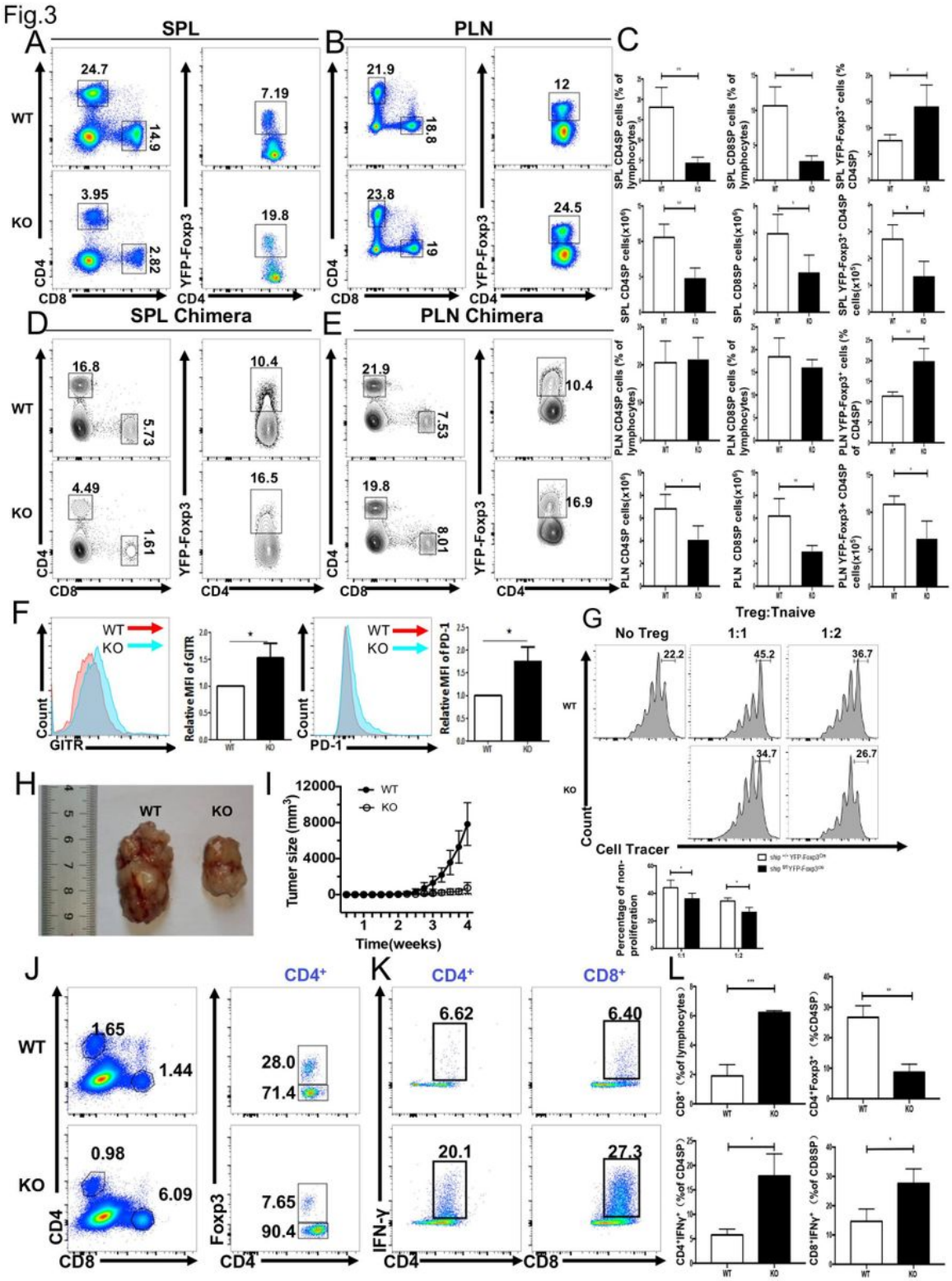

Figure 3

Altered homeostasis and function of SHIP-1 KO Treg cells

(A) Flow cytometry data of CD4SP, CD8SP, and CD4$^+$YFP-Foxp3$^+$ Treg cells from the spleens of WT and SHIP-1 KO mice. (B) Flow cytometry data of CD4SP, CD8SP, and CD4$^+$YFP-Foxp3$^+$ Treg cells in the peripheral lymph nodes of WT and SHIP-1 KO mice (n=6). (C) Percentage and absolute number of

selected cell populations from (A and B) (n=6). (D,E) CD45.1 mice were irradiated with sublethal radiation (6Gy) and intravenously injected with 1×10^7 total BM cells containing WT BM (expressing CD45.1)(n=5) and SHIP-1 KO BM (expressing CD45.2), at a ratio of 1:1. The CD4SP, CD8SP, and $CD4^+$YFP-$Foxp3^+$Treg cells from spleens and peripheral lymph nodes of recipient CD45.1 mice were analyzed after 8 weeks. (F) The expression of GITR and PD-1 in $CD4^+$YFP-$Foxp3^+$Treg cells from spleens of WT and SHIP-1 KO mice (left panel), and the fluorescence intensity ratios of SHIP-1 KO to WT cells (right panel) (n=6). (G) Sorted $CD4^+CD62L^{high}CD44^{low}$ Tnaive cells from wild-type mice(n=4) were labeled with CellTrace Violet, and co-cultured with $CD4^+CD25^+$ Treg cells from WT and SHIP-1 KO mice at a ratio of 1:1, 1:2, or without Treg cells. The proliferation of Tnaive cells was examined by flow cytometry after 3 days. Shown were the representative results from three independent experiments (H) MC38 tumors from WT(n=4) and SHIP-1 KO mice 30 days post-inoculation. (I) Tumor growth curve of WT and SHIP-1 KO mice 30 days post-inoculation. (J) Flow cytometry data of CD4SP, CD8SP, and $CD4^+$ $Foxp3^+$Treg cells from tumor infiltrated lymph nodes of WT and SHIP-1 KO mice. (K) Flow cytometry data of IFN-γ in CD4SP and CD8SP from tumor infiltrated lymph nodes of WT and SHIP-1 KO mice. (L) Percentage of $CD8^+$, $CD4^+Foxp3^+$, $CD4^+IFN\gamma^+$, and $CD8^+IFN\gamma^+$ cells in tumor infiltrated lymph nodes of WT and SHIP-1 KO mice.

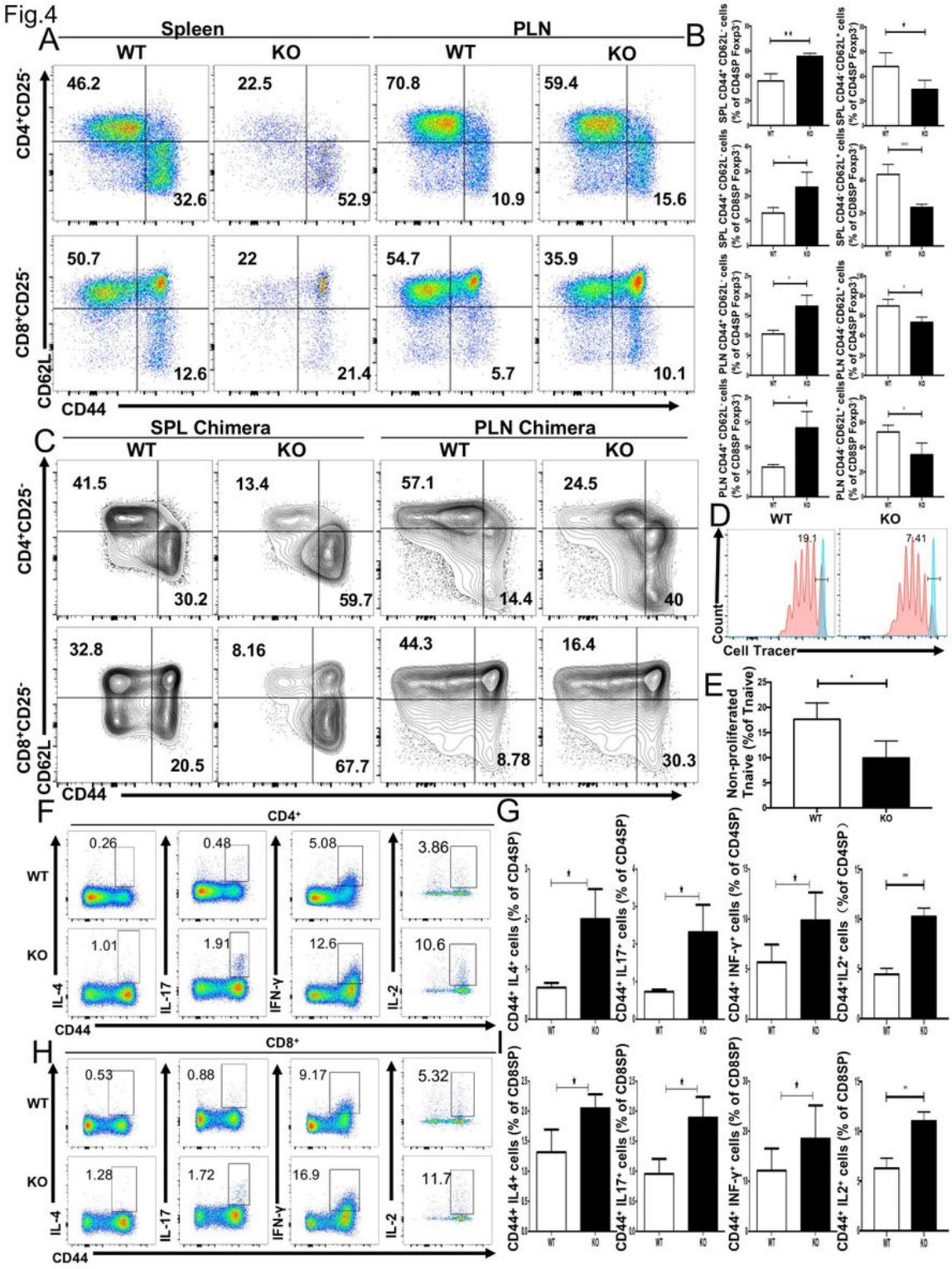

Figure 4

The loss of SHIP-1 in Tregs induces autoimmunity

(A) Flow cytometry data of $CD4^+CD62L^{high}CD44^{low}$ naïve T cells and $CD4^+CD62L^{low}CD44^{high}$ effector or memory T cells in $CD4^+$ or $CD8^+$ T cells from spleens and peripheral lymph nodes of WT and SHIP-1 KO mice. (B) Percentages of selected cell populations from (A) (n=6). (C) CD45.1 mice were irradiated with

sublethal radiation (6Gy) and then intravenously injected with 1×10^7 total BM cells containing SHIP-1 KO BM (expressing CD45.2) and WT BM (expressing CD45.1), at a ratio of 1:1. The $CD4^+CD62L^{high}CD44^{low}$ naïve T cells and $CD4^+CD62L^{low}CD44^{high}$ effector or memory T cells in $CD4^+$ or $CD8^+$ T cells from spleens and peripheral lymph nodes of recipient CD45.1 mice were analyzed after 8 weeks. (D) Sorted $CD62L^{high}CD44^{low}$ naïve T cells from spleens of WT(n=3) and SHIP-1 KO mice were labeled with Cell Trace Violet and stimulated with anti-CD3 and anti-CD28 antibodies for 3 days, then examined for the proliferation of naïve T cells. Shown were the representative results from three independent experiments. (E) Percentage of non-proliferated Tnaive cells from (D). (F) Flow cytometry data of IL-4, IL-17, IL-2, and IFN-γ in $CD4^+CD44^+$ T cells from spleens of WT and SHIP-1 KO mice after stimulation with PMA and ionomycin for 4 hours. (G) Percentages of selected cell populations from (F) (n=6). (H) Flow cytometry analysis of IL-4,IL-17, IL-2, and IFN-γ in $CD8^+CD44^+$ T cells from the spleens of WT and SHIP-1 KO mice after stimulation with PMA and ionomycin for 4 hours. (I) Percentages of selected cell populations from (H) (n=6).

Fig.5

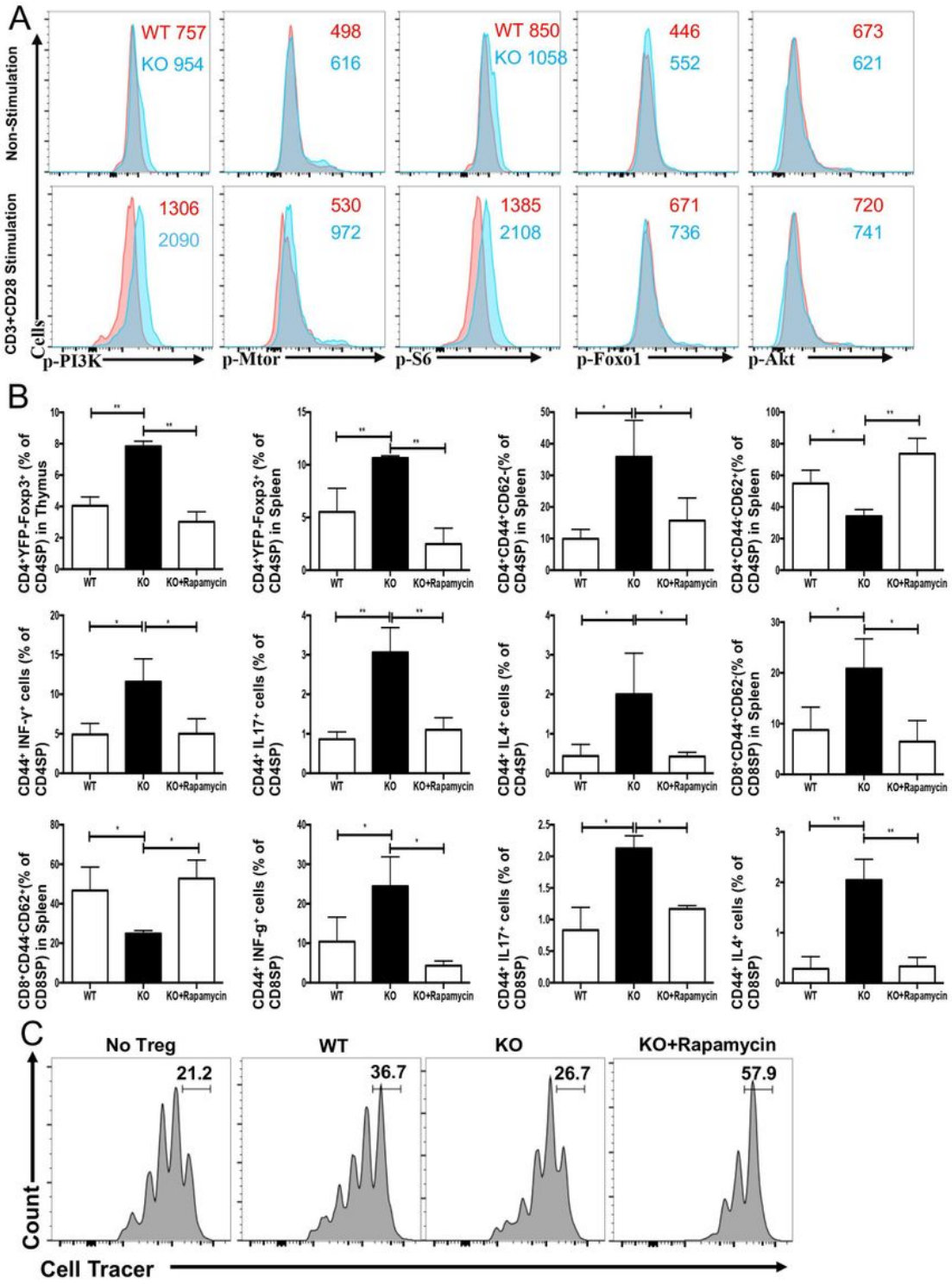

Figure 5

SHIP-1 signaling inhibits mTORC1 to decrease Treg differentiation and function

(A)Flow cytometry analysis of p-S6, p-Mtor, p-Foxo1, p-Akt, and p-Pi3k in $CD4^{+}Foxp3^{+}$Treg cells from WT(n=5) and SHIP-1 KO mice with or without anti-CD3 and anti-CD28 for 4 hours.(B) SHIP-1 KO(n=5) mice were injected with rapamycin by IP injection for 14 consecutive days, then examined for: the

expression of $CD4^+YFP\text{-}Foxp3^+$ in thymocytes and splenocytes, cell populations of $CD4^+CD62L^{high}CD44^{low}$ naïve T cells and $CD4^+CD62L_{low}CD44_{hi}$ effector or memory T cells in $CD4^+$ or $CD8^+$ T cell splenocytes, and the expression of IL-4, IL-17, and IFN-γ in $CD4^+CD44^+$ and $CD8^+CD44^+$T cells after stimulation with PMA and ionomycin for 4 hours. (C) Sorted $CD4^+CD25^+$ Treg cells from untreated WT (n=3) and SHIP-1 KO mice or 1 hr rapamycin-treated SHIP-1 KO mice co-cultured with $CD4^+CD62L^{high}CD44^{low}$ naïve T cells from wild-type mice at a ratio of 1:1. The proliferation of Tnaive cells was examined by flow cytometry after 3 days. Shown were the representative results from three independent experiments.

Supplementary Files

This is a list of supplementary files associated with this preprint. Click to download.

- SupplementaryFigure.pdf